The Astronomical Journal, 127:2352–2361, 2004 April

η CARINAE'S BRIGHTNESS VARIATIONS SINCE 1998: *HUBBLE SPACE TELESCOPE* OBSERVATIONS OF THE CENTRAL STAR[1,2]

J. C. Martin and M. D. Koppelman
Department of Astronomy, University of Minnesota, 116 Church Street, SE, Minneapolis, MN 55455;
michael@aps.umn.edu, martin@aps.umn.edu

and

The *HST* η Carinae Treasury Project Team
Received 2003 November 12; accepted 2004 January 2

ABSTRACT

We have measured the brightness variations in η Carinae for the past 6 years using the *Hubble Space Telescope* (*HST*) Space Telescope Imaging Spectrograph and Advanced Camera for Surveys. Unlike ground-based data, observations by the *HST* allow direct measurement of the brightness of the central star by resolving it from the surrounding bright ejecta. We find interesting behavior during 2003 in the continuum and Hα emission. The data show that the established long-term brightening trend of η Car continues, including regular events that coincide with the 5.5 yr spectroscopic cycle and other more rapid and unexpected variations. In addition to the *HST* data, we also present ground-based data obtained from the American Association of Variable Star Observers that show many of the same features. The dip in the apparent brightness of the central star at the time of the 2003.5 event is wavelength dependent with no decrease in the continuum. These observations cast doubt on a simple eclipse or occultation as the explanation for the dip and place constraints on the models for the event.

Key words: stars: activity — stars: individual (η Carinae)

1. INTRODUCTION

Two unforeseen developments in recent years have made continued photometry of HD 93308 η Car particularly important: distinctive brightness variations in the near-IR accompany its mysterious 5.5 yr spectroscopic cycle (Feast, Whitelock, & Marang 2001; Whitelock et al. 1994), and possibly independent of the cycle (Damineli 1996), the star brightened at a surprising rate after 1997 (Davidson et al. 1999a, 1999b; van Genderen et al. 1999; Sterken et al. 1999). Neither of these phenomena has been explained, and the data since 1998 are seriously incomplete. Meanwhile, the long-term brightening trend continues; for general information about η Car with many references, see Davidson & Humphreys (1997) and Davidson (2000).

Photometry of this bright object is difficult for at least two reasons:

1. At visual wavelengths, normal ground-based observations represent mainly the surrounding "Homunculus" ejecta nebula, which appears much brighter than the central star and has structure at all radii from 0.″2 to 8″. So far the only available measurements of just the central star have been made with the *Hubble Space Telescope* (*HST*). Although the Homunculus is primarily a reflection nebula, its apparent brightness measured with respect to the central star has changed greatly. During 1998–1999, while ground-based observations showed about a 0.3 mag brightening of Homunculus plus star, the star itself nearly tripled in apparent brightness (Davidson et al. 1999a)! This discrepancy presumably involves dust along our line of sight to the star, but as mentioned above, it is only vaguely understood at this time.

2. Numerous strong emission lines produced in the stellar wind perturb the results for standard photometric systems. Hα and Hβ emission, for example, have equivalent widths of about 800 and 180 Å, respectively, in *HST* spectra of η Car. Therefore, broadband *U*, *B*, *R*, and *I* magnitudes, and most medium-band systems as well, are poorly defined for this object. Photometry around 5500 Å, e.g., broadband *V*, is relatively free of strong emission lines, but transformations from instrumental magnitudes to a standard system are imprecise because they involve the other filters (see Davidson et al. 1999a,; Sterken et al. 2001; van Genderen, Sterken, & Allen 2003a, and references therein).

In this paper we report photometry *of the central star* obtained with two *HST* instruments since 1998. For reasons noted above, these observations are quite distinct from all ground-based data, and the star's photometric behavior during 2003 proved to be especially interesting. First we employ acquisition images produced by the Space Telescope Imaging Spectrograph (STIS) because these are numerous and internally reliable; η Car has been observed many times with this instrument since 1998, especially during mid-2003, when the most recent "spectroscopic event" occurred. These broadband red data cannot be transformed to any standard photometric system, but they are quite reliable for showing relative fluctuations by the star (strictly speaking, the stellar wind), uncontaminated by light from the surrounding Homunculus. We also report surprising variations in the star's Hα emission brightness accompanied by measurements of the nearby continuum in the STIS slit-spectroscopy data.

[1] This research was conducted as part of the η Carinae *Hubble Space Telescope* Treasury Project via grant GO-9420 from the Space Telescope Science Institute. *HST* is operated by the Association of Universities for Research in Astronomy (AURA), Inc., under NASA contract NAS 5-26555.

[2] Some of the data presented in this paper were obtained from the Multimission Archive at the Space Telescope Science Institute (MAST). STScI is operated by AURA, Inc., under NASA contract NAS 5-26555. Support for MAST for non-*HST* data is provided by the NASA Office of Space Science via grant NAG 5-7584 and by other grants and contracts. Some of the data presented in this paper were obtained from the American Association of Variable Star Observers International Database.

We supplement the STIS data with similar measurements of a few images obtained in 2002–2003 with the *HST* Advanced Camera for Surveys (ACS). These represent a different set of wavelength bands. Altogether these STIS and ACS results probably represent most of the photometry of η Car that will ever be obtained with the *HST*. Very few additional STIS observations are expected now that the 2003 event has passed. Earlier *HST* FOS, FOC, WFC-PC, and WFPC2 data were not obtained often enough to be suitable for our purposes, and in most cases would be more difficult to compare photometrically for technical reasons. We report the STIS and ACS data now, rather than waiting for two or three more data points in 2004, because the behavior during 2003 was rather unexpected and therefore deserves to be noted promptly.

In addition, we briefly present a convenient summary of η Car's photometric record in the American Association of Variable Star Observers (AAVSO) archives. These "V" magnitudes represent, of course, the entire Homunculus plus star, but they are valuable for comparisons with the *HST* data and also with ground-based photometry using different filter systems reported by, e.g., Feast et al. (2001), van Genderen et al. (1999), Sterken, de Groot, & van Genderen (1996), Whitelock et al. (1994), Fernandez Lajus et al. (2003), and van Genderen et al. (2003b).

In § 2 we present the photometry of the central star based on *HST* STIS acquisition images and the ACS/HRC observations. This is followed by a discussion of the ground-based data from the AAVSO in § 3, and then in § 4 a general discussion about how these results relate to the models that have been presented to describe η Carinae.

2. SPACE-BASED PHOTOMETRY OF THE CENTRAL STAR

Normal ground-based imaging and photometry cannot resolve the central star and small structures in the Homunculus nebula. In this study, we have used the *HST* STIS acquisition images, which have a resolution of about 0.″1, plus the recent ACS/HRC images, which have a resolution of 0.″05, to separate the contribution of the central star from the surrounding nebulously.

2.1. *HST STIS Acquisition Images*

Each set of STIS observations of η Carinae has included a pair of acquisition images. These images are 100×100 pixel subframes (5 arcsec^2) centered on the middle row and column of the CCD (Clampin et al. 1996; Downes et al. 1997; Kim Quijano et al. 2003). Each pair of acquisition images includes an initial targeting image and a postacquisition image. Only the postacquisition images were used to measure the brightness of the central star because the target is rarely well centered in the initial targeting images, which raises concerns about ghost images and internal reflections that may unpredictably affect them (see § 2.1.2).

The majority of the STIS acquisition images of η Car have been taken using the F25ND3 filter, which is a neutral-density filter that covers the wavelengths from 2000 to 11000 Å. Acquisition images using other filters are ignored since they lack significant temporal baseline or coverage, and there is little hope of transforming between filter functions for an object as peculiar as η Car. The F25ND3 filter includes several prominent features in the spectrum of η Car (Fig. 1), and changes in them contribute to any measured brightness variations.

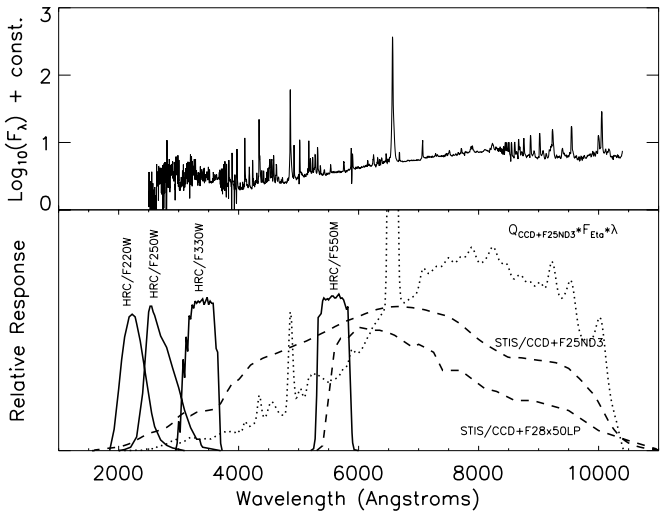

FIG. 1.—*Top*: Relative spectral flux from the central star of η Car. *Bottom*: Total relative response of each CCD and filter combination used in this study, on the same wavelength scale as the top panel. For plotting purposes the curves are not representative of relative responses between filters. STIS filters are plotted with a dashed line and the ACS/HRC filters are plotted with a solid line. The dotted line represents the product of the STIS CCD+F25ND3 response curve and the photon flux from the central star.

2.1.1. *Image Processing and Bias Level Correction*

We processed the STIS acquisition images using the IRAF[3] procedure *stas.hst_calib.stis.basic2d* with version 3.0 of STDAS and version 2.13 of CALSTIS. In lieu of a bias overscan region, each STIS acquisition image has a uniform value of 1510 counts subtracted from each pixel as an approximate bias level correction for the target acquisition process. A small, uncorrected bias level remains in the acquisition images after this initial correction, so we compensate for this tiny effect by modeling it as a function of time and CCD housing temperature.

This residual bias was measured in acquisition images of the standard star AGK +81°266 after the normal bias correction and dark current were subtracted. The exposures of AGK +81°266 are short (2.1 s), and it is more than 60° above the ecliptic, so zodiacal light and other sources make a negligible contribution to the background (Kim Quijano et al. 2003). We found that the residual bias level in the images of AGK +81°266 (Fig. 2) is roughly linear with respect to time prior to the failure of the CCD side-1 controller on 2001 May 16 (Proffitt et al. 2002; Davis et al. 2001). There may be higher order terms in this relation; however, they are not significant in this study since they affect the measurements of the central star by less than 0.001 mag. Subsequent to the failure of the side-1 controller, the STIS CCD temperature regulator has been held at a constant voltage permitting the CCD temperature to fluctuate. As a result, after the side-1 failure the residual bias level of the observations depends on both time and CCD housing temperature. Using the measurements of the residual bias level in the AGK +81°266 observations, the following relations were obtained for the bias level correction as a function of Modified Julian Date (MJD) and CCD housing temperature (T):

[3] IRAF is distributed by the National Optical Astronomy Observatory, which is operated by AURA, Inc., under cooperative agreement with the National Science Foundation.

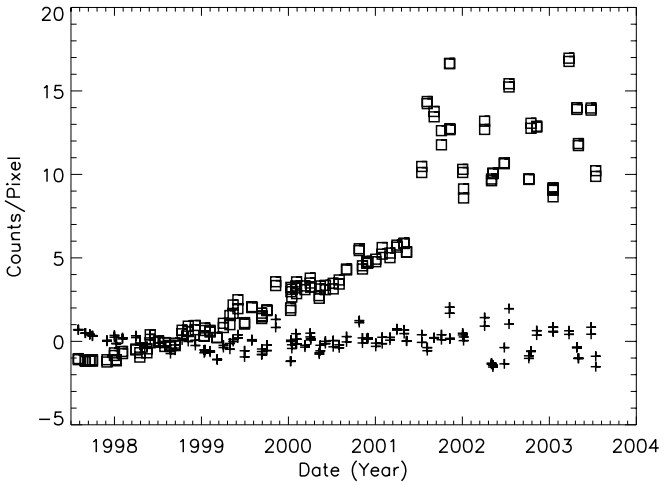

FIG. 2.—Plot of the residual bias level in the 80 STIS acquisition image pairs of flux standard AGK +81°266. Open squares are the residual bias level before subtracting the modeled correction. Plus signs are the bias level after subtracting the modeled correction.

MJD $\leqq$ 52045.5:

$$\mathrm{BLEV} = \begin{cases} -269.84 - 0.0053\ \mathrm{MJD}, & \text{if MJD} \leqq 52045.5 \\ -293.34 - 0.0053\ \mathrm{MJD} - 1.51T, & \text{if MJD} > 52045.5 \end{cases} \quad (1)$$

When the modeled bias level is subtracted from the AGK +81°266 data, the background levels average to -0.03 ± 0.63 counts pixel^{-1} s^{-1} (Fig. 2). This correction was applied to the acquisition images for η Carinae in place of the bias over-scan correction normally implemented in the IRAF BASIC2D procedure. Typically the bias correction amounts to less than 0.005 mag for the measurements reported below.

2.1.2. *Aperture Photometry*

The flux from the central star was measured in each image by summing detector counts within a small, circular virtual aperture. In order to avoid pixelization effects, the counts were weighted by a function of the distance of a pixel from the aperture center (r), which decreases smoothly to zero at the aperture radius R,

$$f(r) = \begin{cases} 1 - r/R^2, & \text{if } r \leq R, \\ 0, & \text{if } r > R. \end{cases} \quad (2)$$

The centering on the star is determined by a peak-up algorithm, which locates the position at which the sum inside the virtual aperture is maximized. For the STIS acquisition images we used $R = 3$ pixels, which corresponds to a diameter of 0.″3 and includes slightly fewer than 30 pixels.

We did not attempt to subtract a background from the measured aperture flux, but this has little effect on the results, since the star provides thousands of counts per pixel per second, far greater than the contribution within the measuring aperture due to scattered and zodiacal light, which contribute only about 0.2 counts pixel^{-1} s^{-1} or less (Kim Quijano et al. 2003). There is no feasible way to account for or remove the contribution from diffuse circumstellar material within 0.″1 of the star. However, STIS spectroscopic data indicate the level of contamination from this source is much smaller than the other uncertainties.

Ghost images exist in the STIS optics but do not contribute significantly to our measurements. When a bright source is centered on the CCD, a ghost image with a peak flux of a few percent relative to the point-spread function (PSF) maximum appears approximately 0.″3 (6 pixels) to the right (increasing column number) of the peak of the PSF. The 0.″3 diameter aperture used to measure the central star excludes this ghost. However, any future work that attempts to measure the flux from the nebula immediately surrounding the central star in these images must confront this problem.

The reduction procedure was tested using 80 pairs of acquisition images of the flux standard AGK +81°266 (Fig. 3). The measured aperture photometry for this standard shows a constant level with an rms scatter of ± 0.037 mag. It should be noted that AGK +81°266 was observed using the F28 × 50LP "long-pass" filter rather than the F25ND3 filter, which was used for the η Car observations. At the same time, the gross spectral energy distribution of AGK +81°266 (spectral class B5) and η Car are very dissimilar. This is not significant, since AGK +81°266 is only used to demonstrate that this method accurately measures a constant brightness over the temporal baseline for an established flux standard. The brightness of η Car is *not* measured relative to AGK +81°266.

2.1.3. *Results*

In Figure 4 and Table 2 we present our results for the STIS acquisition images as instrumental magnitudes calibrated for long-term sensitivity effects using the photometric constants calculated by the reduction pipeline (Kim Quijano et al. 2003) and scaled relative to the value on 1999 February 20 (1999.14). These represent an extremely broadband wavelength sample (Fig. 1). For the purpose of comparison with familiar photometric systems, Table 1 gives approximate Johnson V (Johnson & Morgan 1953) and Cousins R and I (Cousins 1976) magnitudes at the reference epoch (1999.14). These were calculated using flux-calibrated STIS spectroscopic data (K. Davidson 2003, private communication), a flux-calibrated spectrum of Vega (Colina, Bohlin, & Castelli 1996), and the appropriate response functions (Johnson & Morgan 1951; Bingham & Cousins 1974). For reasons noted in § 1 and uncertainties in the STIS slit throughput for an object that is not exactly a point source, entries for η Car in Table 1 probably have uncertainties of roughly ± 0.05 mag and could possibly be somewhat worse. It is also possible that the photometric color may trend mildly blueward as the object brightens (Davidson et al. 1999a).

The Homunculus is currently of fifth magnitude according to *ground-based* Johnson V photometry (§ 3 below), but the central star is fainter than $V = 7.0$ as stated in Table 1. Its apparent continuum is red, while stellar wind emission lines contribute a significant fraction of its brightness. In the 1999.14 spectrum, Hα and other emission features contribute about 16% of the

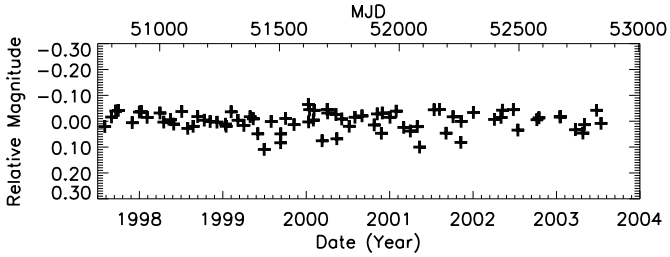

FIG. 3.—Relative brightness of flux standard AGK +81°266 measured using a 0.″3 diameter weighted aperture.

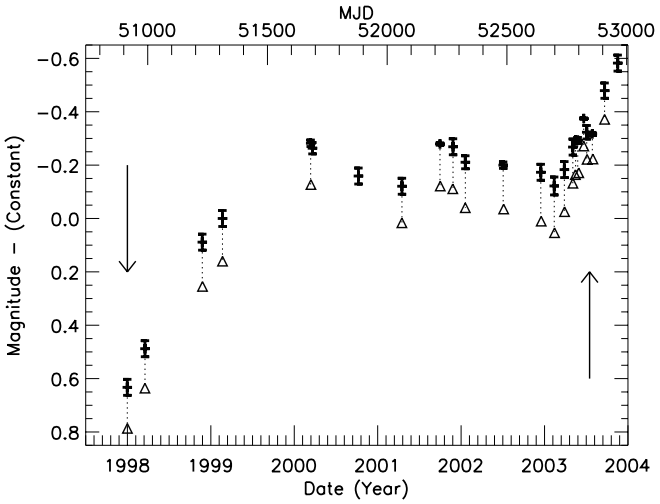

FIG. 4.—Plus signs with error bars are the average relative brightness of the central star in the STIS acquisition images (Table 2). The error bars are the 1 σ standard deviation of the measurements included in each point. The error bars plotted for points including only one measurement are the rms deviation of the brightness measured for the flux standard AGK +81°266. The open triangles are the magnitudes with the contribution of Hα subtracted. Vertical arrows mark the times of the 1998.0 and 2003.54 spectroscopic events. See Fig. 6 for an expanded view of the data around the 2003.5 event.

flux in V (4% from Hα) and 38% of the flux in R (35% from Hα). Meanwhile, there is about a 5% effect on the I flux from the hydrogen Paschen lines, which are in emission. Because these emission features are constantly changing, it is not possible to formulate a consistent set of transformations to convert the STIS magnitudes to the more familiar Johnson V and Cousins R and I magnitudes for η Car. However, the values presented for 1999.14 can serve as a rough zero point.

Figure 4 shows that the dramatic brightening reported by Davidson et al. (1999a) leveled off by 2000, but may have resumed at least temporarily around the mid-2003 spectroscopic event. The dip in brightness near the time of the event (Fig. 6) may be reminiscent of the near-infrared behavior reported by Feast et al. (2001). This is discussed further in § 4.

2.1.4. *Concerning* Hα *Emission*

The broad Hα emission of η Car, produced in the stellar wind at radii of several AU, is tremendously strong (equivalent width usually about 800 Å). This feature did not vary much relative to the continuum in STIS data from 1998 to 2002, but recently it has faded to a surprising degree, as reported below. Since Hα contributes appreciably to the STIS acquisition images, we have investigated the effects on our photometry.

K. Davidson (2003, private communication) has measured the equivalent width of Hα and estimated the absolute level of the nearby continuum in short-exposure STIS slit data. Hα was integrated from 6509 to 6650 Å, and the continuum flux was averaged between 6740 and 6800 Å (an interval that is practically uncontaminated by emission lines). These continuum measurements have the advantage of being approximately calibrated in physical units, but on the other hand, they may be underestimated if the slit was not perfectly centered on the star. Fortunately, the Hα equivalent width measurements are quite insensitive to slit position. The results are shown in Figure 5. We estimate that Hα contributes from 8% to 16% of the STIS/F25ND3 counts, varying with time as listed in Table 2. Open triangles in Figure 4 represent the instrumental magnitudes that would have been observed if Hα were not present; evidently the brightness minimum in early 2003 and the subsequent rapid brightening are not due to this emission line. The measured brightness fluctuations in the central star appear to be mainly (though not entirely) changes in the continuum brightness.

In the 6 months preceding the 2003.5 event (2002 December to 2003 June), the equivalent width of Hα declined by a factor of nearly 2, while its line profile evolved in an interesting and unexpected way, which is beyond the scope of this paper. The other Balmer lines behaved in a similar fashion. Moreover, in 2003 July and September they did not return to the state observed by STIS in 1998 at the corresponding point in η Car's 5.54 yr cycle. A more in-depth account of these effects will be reported in a paper that is now in preparation (Davidson et al. 2004).

TABLE 1
BRIGHTNESS OF THE CENTRAL STAR AT 1999.140

Source	V_J	R_C	I_C
η Car	7.73	6.11	4.47
Vega.....	0.030	0.021	0.025

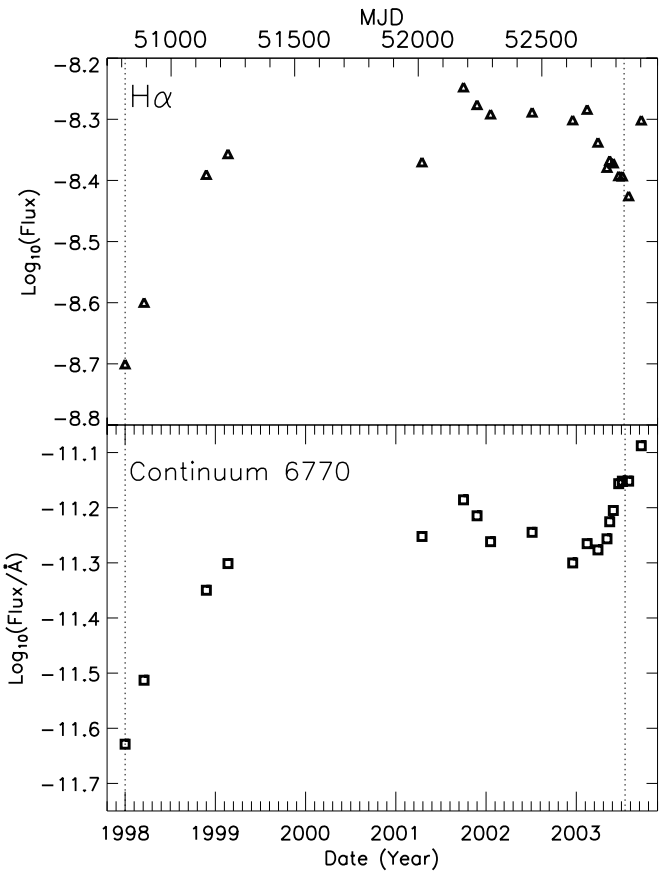

FIG. 5.—Flux of features in the STIS spectrum of the central star. *Top*: The log of the total integrated flux of Hα in ergs cm^{-2} s^{-1}. Bottom: The log of the continuum flux measured at 6770 Å in ergs cm^{-2} s^{-2} Å^{-2}. The dotted vertical lines mark the spectroscopic events at 1998.0 and 2003.54.

TABLE 2
RESULTS FROM STIS ACQUISITION IMAGES

Data Set	MJD	Year	Flux[a]	Hα[b] (%)	Flux at 6770 Å	Magnitude[d]	Average[e]	σ[e]	Minus Hα[f]
o4j802qxq	50814.008	1997.999	3.196E−12	13.2	2.35E−12	0.65	0.65	...	0.79
o4j801y4q	50891.414	1998.211	3.720E−12	12.7	3.07E−12	0.49	0.49	...	0.64
o55601hkq.....	51142.172	1998.898	5.374E−12	14.2	4.47E−12	0.09	0.09	...	0.25
o55602qsq.....	51230.449	1999.140	5.831E−12	13.7	5.00E−12	−0.00	−0.00	...	0.16
o5f102bkq	51616.484	2000.197	7.476E−12	13.3	...	−0.27	−0.28	0.01	−0.13
o5kz01coq.....	51623.785	2000.217	7.645E−12	...	...	−0.29	...	...	...
o5kz02gbq.....	51624.285	2000.218	7.580E−12	...	...	−0.28	−0.26	0.02	...
o5f101yoq	51626.762	2000.225	7.288E−12	...	...	−0.24	...	...	...
o5f103a1q	51826.039	2000.769	6.753E−12	...	...	−0.16	−0.16	...	...
o62r01h0q	52016.734	2001.291	6.518E−12	11.9	5.60E−12	−0.12	−0.12	...	0.02
o6ex03a9q.....	52183.086	2001.747	7.573E−12	13.5	6.52E−12	−0.28	−0.28	0.00	−0.12
o6en01c2q.....	52183.297	2001.747	7.509E−12	...	...	−0.27	...	...	...
o62r02fvq.....	52240.070	2001.903	7.470E−12	13.5	6.10E−12	−0.27	−0.27	...	−0.11
o6ex02tkq.....	52293.977	2002.051	7.241E−12	14.5	5.47E−12	−0.24	−0.21	0.02	−0.04
o6ex01wyq.....	52294.207	2002.051	6.923E−12	...	...	−0.19	...	...	...
o6mo02eaq.....	52459.480	2002.504	6.933E−12	14.1	5.69E−12	−0.19	−0.20	0.01	−0.04
o6mo01k6q	52459.781	2002.505	7.089E−12	...	...	−0.21	...	...	...
o8gm01a1q.....	52624.043	2002.955	6.840E−12	15.5	5.01E−12	−0.17	−0.17	...	0.01
o8gm12ukq	52682.859	2003.116	6.730E−12	14.9	5.43E−12	−0.16	−0.12	0.03	0.05
o8gm11zpq.....	52683.242	2003.117	6.326E−12	...	...	−0.09	...	...	...
o8gm21t9q	52727.234	2003.238	6.904E−12	13.5	5.29E−12	−0.18	−0.18	...	−0.03
o8gm41eqq.....	52764.266	2003.339	7.462E−12	11.7	5.54E−12	−0.27	−0.27	...	−0.13
o8gm33qsq.....	52776.398	2003.372	7.662E−12	11.2	5.95E−12	−0.30	−0.29	0.00	−0.16
o8gm32c6q.....	52778.469	2003.378	7.623E−12	...	...	−0.29	...	...	...
o8gm31fnq.....	52785.797	2003.398	7.617E−12	10.6	6.24E−12	−0.29	−0.29	0.01	−0.17
o8gm51fuq.....	52791.035	2003.412	7.752E−12	...	...	−0.31	...	...	...
o8gm52kyq	52791.707	2003.414	7.558E−12	...	...	−0.28	...	...	...
o8gm63ohq	52812.031	2003.470	8.264E−12	9.0	6.98E−12	−0.38	−0.37	0.00	−0.27
o8gm61pxq	52812.250	2003.471	8.212E−12	...	...	−0.37	...	...	...
o8gm62dwq.....	52813.703	2003.475	8.222E−12	...	...	−0.37	...	...	...
o8ma71jnq.....	52825.020	2003.506	7.675E−12	8.9	7.05E−12	−0.30	−0.32	0.03	−0.22
o8ma72liq.....	52825.355	2003.506	8.043E−12	...	...	−0.35	...	...	...
o8ma81mtq.....	52849.594	2003.573	7.763E−12	8.3	7.05E−12	−0.31	−0.32	0.01	−0.22
o8ma82b8q.....	52851.906	2003.579	7.850E−12	...	...	−0.32	...	...	...
o8ma91ubq.....	52903.355	2003.720	8.830E−12	...	...	−0.45	−0.48	0.03	...
o8ma92ctq.....	52904.289	2003.723	9.309E−12	...	...	−0.51	...	...	...
o8ma83fzq.....	52960.590	2003.877	9.969E−12	...	...	−0.58	...	...	...

[a] Brightness measured in F25ND3 filter given as STIS flux units (ergs cm^{-2} s^{-1} $Å^{-1}$).
[b] An estimate of the percentage of the total flux measured in the F25ND3 filter that is contributed by Hα.
[c] The continuum flux measured at 6770 Å in absolute flux units of ergs cm^{-2} s^{-1} $Å^{-1}$.
[d] Relative STIS magnitude in the F25ND3 filter zeroed on 1999.140.
[e] The average and sigma of individual measurements within 1 day of each other. These values are plotted in Fig. 4.
[f] Relative magnitude in the F25ND3 filter with the contribution from Hα subtracted (Fig. 4, *open triangles*).

2.2. *ACS/HRC Observations*

HST ACS/HRS observations of η Car were obtained for the *HST* Treasury Project beginning in October 2002. Bias-corrected, dark-subtracted, and flat-fielded ACS/HRC images were obtained from Space Telescope Science Institute via the Multi-Mission Archive (MAST).[4] Observations that had over-exposed the central star were not used, and no drizzle or dithering correction is applied.

The ACS/HRC images were taken in four filters that cover near-UV and optical wavelengths (Fig. 1). Each of these filters is influenced by different types of spectral features. The UV filters (HRC/F220W and HRC/F250W) are heavily influenced by the "Fe II forest" (Cassatella, Giangrande, & Viotti 1979; Altamore et al. 1986; Viotti et al. 1989). The opacity of this "forest" is known to dramatically increase during an event (Davidson et al. 1999c; Gull, Davidson, & Ishibashi 2000). The HRC/F330W filter is sensitive to both the Balmer continuum and a number of emission features while the HRC/F550M filter, strategically placed between Hα and Hβ, almost exclusively measures the continuum.

The relative brightness of the central star in the ACS/HRC images is measured with the same weighted 0.″3 diameter aperture used to measure the STIS acquisition images. On the scale of the ACS/HRC this corresponds to $R = 5$ pixels and includes about 79 pixels inside the aperture. The results are given in Table 3 and Figure 6. The magnitudes given are on the STMAG system (Holtzman et al. 1995) as calibrated by the photometric keywords calculated by the reduction pipeline (Pavlovsky et al. 2003). Note that the HRC/F220W and HRC/F250W curves show a significant dip at the time of the 2003.5 event, due to the Fe II absorption as noted above.

[4] See http://archive.stsci.edu.

TABLE 3

RESULTS FROM ACS/HRC IMAGES

Data Set	MJD	Year	Flux (ergs cm^{-2} s^{-1} Å^{-1})	Magnitude[a]	Average[b]	σ[b]
			HRC/F220W Filter			
j8gm1aa7q.....	52561.039	2002.782	1.385E−12	8.547	8.549	0.011
j8gm1aa8q.....	52561.039	2002.782	1.402E−12	8.533	...	...
j8gm1aalq.....	52561.047	2002.782	1.366E−12	8.562	...	...
j8gm1aamq.....	52561.047	2002.782	1.375E−12	8.554	...	...
j8gm1abmq.....	52561.098	2002.782	1.426E−12	8.515	8.535	0.015
j8gm1abnq.....	52561.098	2002.782	1.404E−12	8.531	...	...
j8gm1abyq.....	52561.105	2002.782	1.394E−12	8.539	...	...
j8gm1abxq.....	52561.105	2002.782	1.374E−12	8.555	...	...
j8gm2as1q.....	52682.547	2003.115	1.562E−12	8.416	8.417	0.007
j8gm2as5q.....	52682.551	2003.115	1.574E−12	8.407	...	...
j8gm2asaq.....	52682.555	2003.115	1.555E−12	8.421	...	...
j8gm2asoq.....	52682.566	2003.115	1.549E−12	8.425	...	...
j8ma3adhq.....	52803.055	2003.445	1.316E−12	8.601	8.571	0.018
j8ma3adlq.....	52803.086	2003.445	1.372E−12	8.557	...	...
j8ma3adqq.....	52803.090	2003.445	1.373E−12	8.556	...	...
j8ma3ae3q.....	52803.152	2003.446	1.355E−12	8.570	...	...
j8ma4aqfq.....	52840.145	2003.547	8.093E−13	9.130	9.129	0.003
j8ma4aqj	52840.148	2003.547	8.069E−13	9.133	...	...
j8ma4aqnq.....	52840.156	2003.547	8.109E−13	9.128	...	...
j8ma4ar2q.....	52840.168	2003.547	8.137E−13	9.124	...	...
j8ma6ayjq.....	52957.809	2003.869	9.216E−13	8.989	8.970	0.01
j8ma6aynq.....	52957.844	2003.869	9.531E−13	8.952	...	...
j8ma6az2q.....	52957.855	2003.869	9.385E−13	8.969	...	...
			HRC/F250W Filter			
j8gm1aaaq.....	52561.039	2002.782	2.935E−12	7.731	7.726	0.011
j8gm1aabq.....	52561.043	2002.782	2.995E−12	7.709	...	...
j8gm1aaoq.....	52561.047	2002.782	2.910E−12	7.740	...	...
j8gm1aapq.....	52561.051	2002.782	2.951E−12	7.725	...	...
j8gm1abpq.....	52561.098	2002.782	2.985E−12	7.713	7.722	0.018
j8gm1abqq.....	52561.098	2002.782	3.022E−12	7.699	...	...
j8gm1ac0q.....	52561.105	2002.782	2.895E−12	7.746	...	...
j8gm1ac1q.....	52561.105	2002.782	2.937E−12	7.730	...	...
j8gm2as2q.....	52682.547	2003.115	3.181E−12	7.643	7.646	0.006
j8gm2as6q.....	52682.551	2003.115	3.198E−12	7.638	...	...
j8gm2ascq	52682.559	2003.115	3.174E−12	7.646	...	...
j8gm2asqq.....	52682.570	2003.115	3.148E−12	7.655	...	...
j8ma3adiq.....	52803.055	2003.445	3.058E−12	7.687	7.651	0.021
j8ma3admq.....	52803.086	2003.445	3.194E−12	7.639	...	...
j8ma3adsq	52803.094	2003.445	3.184E−12	7.642	...	...
j8ma3ae5q.....	52803.156	2003.446	3.208E−12	7.634	...	...
j8ma4aqgq.....	52840.148	2003.547	2.178E−12	8.055	8.063	0.008
j8ma4aqkq.....	52840.152	2003.547	2.137E−12	8.076	...	...
j8ma4aqpq.....	52840.156	2003.547	2.171E−12	8.058	...	...
j8ma4ar4q.....	52840.168	2003.547	2.159E−12	8.065	...	...
j8ma6aqgq.....	52957.805	2003.869	2.619E−12	7.855	7.840	0.015
j8ma6aykq.....	52957.809	2003.869	2.628E−12	7.851	...	...
j8ma6aypq.....	52957.848	2003.869	2.710E−12	7.817	...	...
j8ma6az4q.....	52957.859	2003.869	2.664E−12	7.836	...	...
			HRC/F330W Filter			
j8gm1aacq.....	52561.043	2002.782	3.306E−12	7.602	7.621	0.014
j8gm1aadq.....	52561.043	2002.782	3.253E−12	7.619	...	...
j8gm1aaqq.....	52561.051	2002.782	3.243E−12	7.623	...	...
j8gm1aarq.....	52561.051	2002.782	3.189E−12	7.641	...	...
j8gm1abrq	52561.098	2002.782	3.378E−12	7.578	7.608	0.021
j8gm1absq.....	52561.102	2002.782	3.292E−12	7.606	...	...
j8gm1ac2q.....	52561.105	2002.782	3.273E−12	7.612	...	...
j8gm1ac3q.....	52561.109	2002.782	3.201E−12	7.637	...	...
j8gm2as3q.....	52682.547	2003.115	3.327E−12	7.595	7.598	0.002
j8gm2as7q.....	52682.551	2003.115	3.312E−12	7.600	...	...

TABLE 3—*Continued*

Data Set	MJD	Year	Flux (ergs cm^{-2} s^{-1} Å^{-1})	Magnitude[a]	Average[b]	σ[b]
j8gm2asgq.....	52682.563	2003.115	3.313E−12	7.599	...	...
j8ma3adjq.....	52803.055	2003.445	3.913E−12	7.419	7.379	0.023
j8ma3adnq.....	52803.090	2003.445	4.095E−12	7.369	...	...
j8ma3adwq.....	52803.098	2003.445	4.112E−12	7.365	...	...
j8ma3ae9q.....	52803.160	2003.446	4.119E−12	7.363	...	...
j8ma4aqhq.....	52840.148	2003.547	3.671E−12	7.488	7.494	0.003
j8ma4aqlq.....	52840.152	2003.547	3.649E−12	7.495	...	...
j8ma4aqtq.....	52840.160	2003.547	3.648E−12	7.495	...	...
j8ma4ar8q.....	52840.176	2003.547	3.642E−12	7.497	...	...
j8ma6aqhq.....	52957.805	2003.869	4.643E−12	7.233	7.222	0.008
j8ma6aylq.....	52957.809	2003.869	4.695E−12	7.221	...	...
j8ma6aytq.....	52957.852	2003.869	4.738E−12	7.211	...	...
j8ma6az8q.....	52957.852	2003.869	4.678E−12	7.225	...	...
HRC/F550M Filter						
j8gm1aafq.....	52561.043	2002.782	3.700E−12	7.479	7.485	0.006
j8gm1aatq.....	52561.051	2002.782	3.663E−12	7.491	...	...
j8gm1abuq.....	52561.102	2002.782	3.755E−12	7.463	7.475	0.014
j8gm1ac5q.....	52561.109	2002.782	3.649E−12	7.494	...	...
j8gm1ac4q.....	52561.109	2002.782	3.745E−12	7.466	...	...
j8gm2as4q.....	52682.551	2003.115	4.129E−12	7.360	7.359	0.004
j8gm2as8q.....	52682.555	2003.115	4.162E−12	7.352	...	...
j8gm2asjq.....	52682.566	2003.115	4.134E−12	7.359	...	...
j8gm2asxq.....	52682.578	2003.115	4.118E−12	7.363	...	...
j8ma3adkq.....	52803.059	2003.445	4.963E−12	7.161	7.126	0.020
j8ma3adoq.....	52803.090	2003.445	5.156E−12	7.119	...	...
j8ma3adzq.....	52803.102	2003.445	5.168E−12	7.117	...	...
j8ma3aecq	52803.164	2003.446	5.206E−12	7.109	...	...
j8ma4aqiq.....	52840.148	2003.547	5.259E−12	7.098	7.099	0.003
j8ma4aqmq.....	52840.152	2003.547	5.250E−12	7.100	...	...
j8ma4aqwq	52840.164	2003.547	5.234E−12	7.103	...	...
j8ma4arbq.....	52840.180	2003.547	5.272E−12	7.095	...	...
j8ma6ayiq.....	52957.805	2003.869	6.851E−12	6.811	6.807	0.004
j8ma6aymq.....	52957.813	2003.869	6.907E−12	6.802	...	...
j8ma6aywq.....	52957.855	2003.869	6.890E−12	6.804	...	...
j8ma6azbq.....	52957.867	2003.869	6.849E−12	6.811	...	...

[a] Magnitude on the STMAG system.
[b] The average and standard deviation of individual measurements in an exposure set. These values are plotted in Fig. 6.

Interestingly, the visual continuum measured by the HRC/F550M filter does *not* show the decrease in brightness seen at longer wavelengths in the STIS data.

3. GROUND-BASED AAVSO DATA

While space-based photometry is able to resolve the central star, ground-based photometry measures the integrated brightness of both the star and the Homunculus nebula. However, ground-based photometry is still valuable because it has a longer temporal baseline and shows many of the same brightness variations, albeit at different amplitudes. Also, as more publicly funded small telescopes are closed, the data from the AAVSO and groups such as the La Plata observatory (Fernandez Lajus et al. 2003) will become increasingly useful for monitoring objects like η Car.

One of the few sources for long-term monitoring of η Car is the AAVSO (Mattei & Foster 1998). From 1968 through mid-2003 there were 6640 observations from 110 observers situated around the globe.[5] These data are from individual observers who have determined the brightness of η Car by visually comparing it with the brightness of other stars. Ten observers account for 69% of these observations, while 36% of the observations are from the two most prolific observers: M. Daniel Overbeek (Mattei & Fraser 2003) and Albert F. Jones. On average there are 60 observations per observer, but the median is nine observations per observer.

We averaged the observations in 90 day bins with a median of 32 observations in each bin. The bottom panel of Figure 7 shows binned averages from 1968 through mid-2003, with a typical standard deviation of 0.2 mag, which is consistent with the accepted usual rms error of 0.1–0.2 mag for observations of this type. The top panel of Figure 7 shows the photoelectric Johnson V band photometry (PEPV) from Stan Walker (Davidson et al. 1999a), photoelectric observations from R. Winfield Jones obtained through the AAVSO, and the average V_J magnitude from ground-based observations reported in Figure 2 of Davidson et al. (1999a). The data in both panels follow the same general trend and compare well with the data presented in Figure 2 of Sterken et al. (1996). Even the most primitive AAVSO data track the professional photometry well enough to show irregular behavior. The maximum noted by

[5] See http://www.aavso.org/news/etacar.shtml.

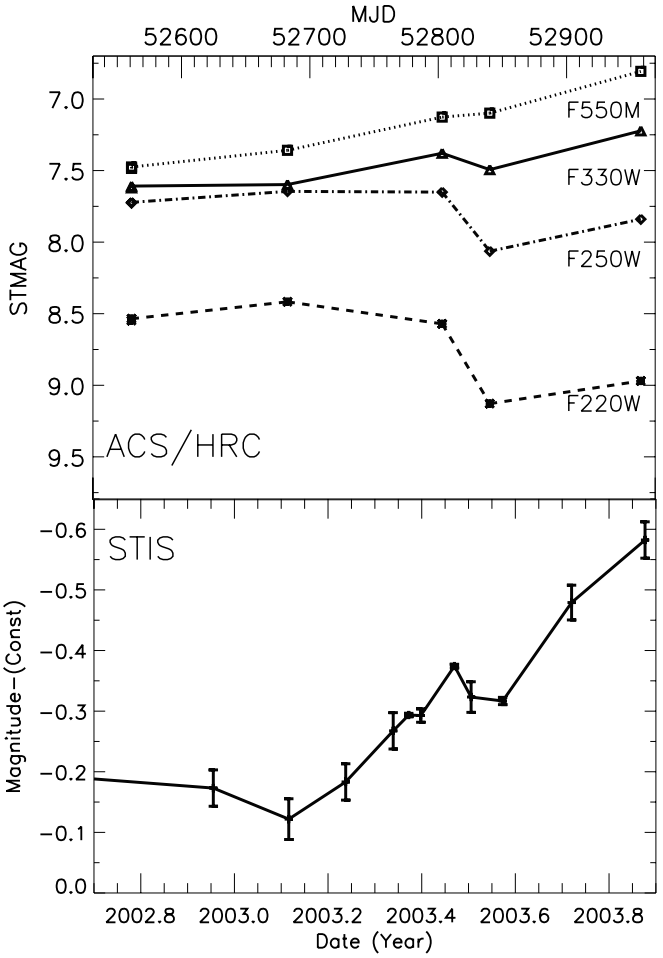

FIG. 6.—*Top*: Brightness of the central star in the ACS/HRC images with each point representing the average of several individual exposures (Table 3). The data for each filter is represented as its own line, labeled on the right. *Bottom*: Data from the STIS acquisition images.

Sterken et al. (1996) at 1982.11 is visible in all the data, although the errors in the binned AAVSO data make it harder to recognize. Each data set also shows an overall brightening trend in η Car over the past 30 years along with a notable jump in brightness in 1998–1999 (Davidson et al. 1999a).

The binned AAVSO data for the last 5 years (Fig. 8) also follows a trend similar to the brightness variations in the central star measured from the STIS acquisition images (Fig. 4). Of particular note, both data sets show that the brightening of η Car peaked in 2000, fell off a bit, and then peaked again in early 2002 before brightening through the 2003.5 event.

4. ANALYSIS AND CONCLUSIONS

The data presented here from the *HST* and ground-based observations confirm the dramatic brightening in both the nebula and central star of η Car, which was previously reported by Davidson et al. (1999a, 1999b) and Sterken et al. (1999), along with a more gradual brightening spanning the past 30 years. All the available data also show that the apparent brightness of η Car fluctuates with no obvious period. We also see intervals (on the order of months) with short-lived increases in apparent brightness similar to those reported by van Genderen et al. (2003a). The 2003.5 event, as observed in the brightness fluctuations of the central star at visual wavelengths, was characterized by a roughly 6 month rise, then a sharp dip in most filters, followed by a recovery to the highest flux observed for the central star in recent years, which may be the start of another significant brightening episode. Again we emphasize that since 1997 *the central star has brightened substantially faster than the Homunculus* (compare Figs. 4 and 7).

The STIS, ACS, Hα, and AAVSO data all have notable trends that began about 200 days before the 2003.54 event. The visual-band photometry from the STIS, ACS, and AAVSO began to brighten significantly in January 2003 (Figs. 9 and 6 and also Fernandez Lajus et al. 2003), which coincided with a steep drop in Hα luminosity (Fig. 5) and the beginning of a dip in brightness in the near-UV (Fig. 6). The start time for this pre-event activity is important because most models that invoke a binary companion to trigger the events place the secondary on a very eccentric orbit that places it in close proximity to the primary for only a very brief period of time during each cycle. Feast et al. (2001) showed that the *J*, *H*, *K*, and *L* bands brightened roughly 500 days before the time of the events over the past two decades, with an additional sharp rise in the *J*, *H*, and *K* bands about 80 days prior to the 1998.0 event. The X-ray flux from η Car (see Ishibashi et al. 1999 and

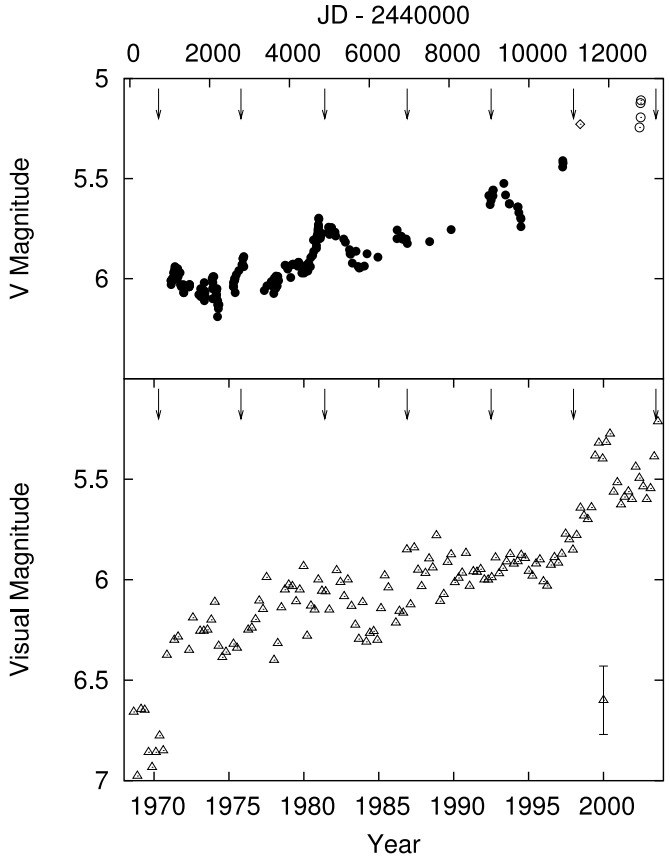

FIG. 7.—Light curve of η Car from ground-based observations. *Top*: Photoelectric *V* magnitudes (PEPV) from Stan Walker (*filled circles*), photoelectric *V* observations by *R*. Winfield Jones obtained from the AAVSO (*open circles*), and the average V_J magnitude from the ground-based observations reported by Davidson et al. (1999c; *open diamonds*). *Bottom*: Averages of the visual AAVSO observations in bins of 90 days. A representative error bar for the binned AAVSO observations is shown in the lower right; see also Fig. 8. The arrows along the top of each panel mark the interval of past events with the 5.54 yr period adopted in 2001 for the Treasury Project proposal. This period was based on photometric details reported by Feast et al. (2001) and various other data, and it predicted the timing of the 2003 event quite well.

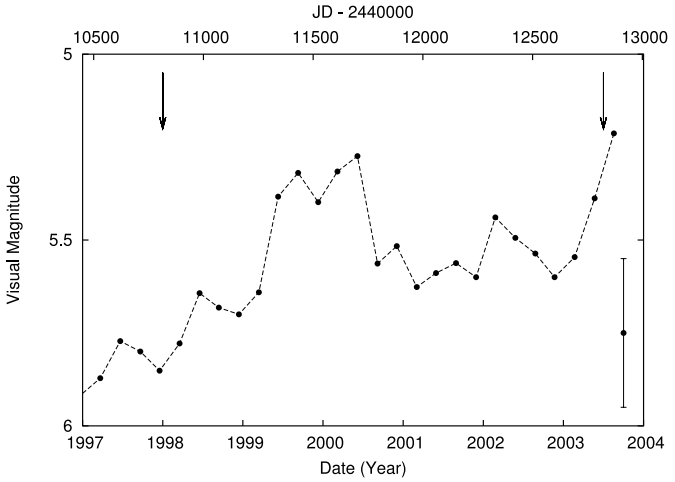

FIG. 8.—Light curve for η Car from 1997 through 2003 of the visual AAVSO observations averaged in bins of 90 days. A representative error bar for a single observation is shown at the lower right; each point here typically represents about 32 observations. The arrows at the top of the plot mark the 1998.0 and 2003.54 spectroscopic events. Formal error estimates are not fully justified in this case, but the rms uncertainty for each plotted point is probably about 20% as large as the single-observation error bar.

M. Corcoran's Web page for data on the recent event)[6] also increased before the 1998.0 and 2003.54 events, preceding them by about 350 and 700 days, respectively. It is not necessary or expected that all of the pre-event activity will temporally coincide since each of these data measure activity that occurs at different radii from the star and a shock front that pushes deeper as the event proceeds will not affect each process simultaneously. Also, as noted below, there is compelling evidence that the state and distribution of the material immediately surrounding the central star has evolved over time, so that while the activity prior to the event should maintain roughly the same sequential order, the exact start times relative to the event could potentially change from cycle to cycle.

The ACS/HRC data show that the brief dip in apparent brightness during the 2003.5 event is not achromatic. The ACS data show that the depth of the dip is wavelength dependent; the dip is deeper at shorter wavelengths and the brightness increases continually in the HRC/F550M filter through the last data point. However, Feast et al. (2001) showed that the brief decrease or dip in luminosity occurred at all of the near-IR wavelengths during the 1998.0 event (Fig. 9, reproduced from Feast et al. 2001), and Whitelock, Marang, & Crause (2003) reported similar activity during the 2003.5 event. This leaves two possibilities, which are not mutually exclusive:

1. the decrease in brightness occurs later at redder wavelengths, and/or
2. the decrease in brightness is driven entirely by increased line opacities, decreased emission lines, and Balmer and Paschen continua formed in the wind, rather than a change in the star's continuum flux.

Feast et al. (2001) show that during the 1998.0 event, the dip in the *J* band occurred about 35 days later than the dip in the X-ray. They also note that the epoch of the minimum in the dip increases slightly with increasing effective wavelength (Fig. 9). Whitelock et al. (2003) reported that during the 2003.5 event the dip in the *J* and *L* bands began sometime between MJD 52809.5 (2003.467) and 52814.5 (2003.481), which preceded the observed dip in Johnson-Cousins *BVRI* by about 1–2 weeks (Fernandez Lajus et al. 2003; van Genderen et al. 2003b). (Note that wavelengths around 2 μm observed by Feast et al. [2001] presumably represent free-free emission in the wind at radii substantially larger than the photosphere at visual wavelengths.) Given only the *HST* data, one might suspect that dip in the HRC/F550M filter may have occurred between data points and the slight rise observed at MJD 52803.1 (2003.45) is the rise in luminosity that precedes the dip. However, the HRC/550M observation at MJD 52840.1 (2003.55) shows a *rise* in flux roughly coincident with the minimum observed in *BVRI* by Fernandez Lajus et al. (2003) and van Genderen et al. (2003b). Therefore, it is unlikely that we missed the dip in HRC/550M because of sampling.

Likewise, strong P Cygni absorption is present in the hydrogen lines during the event (Davidson et al. 1999c). Since the hydrogen emission lines contribute significantly to the total brightness of the central star, anything that changes their profiles will change the brightness measured in a filter that they influence. The HRC/F550M filter covers none of the prominent emission lines, and it shows no dip concurrent with the dip in the other filters. Therefore, this may indicate that the bolometric luminosity of the central star is largely unaffected by the mechanism that causes the observed decrease in brightness.

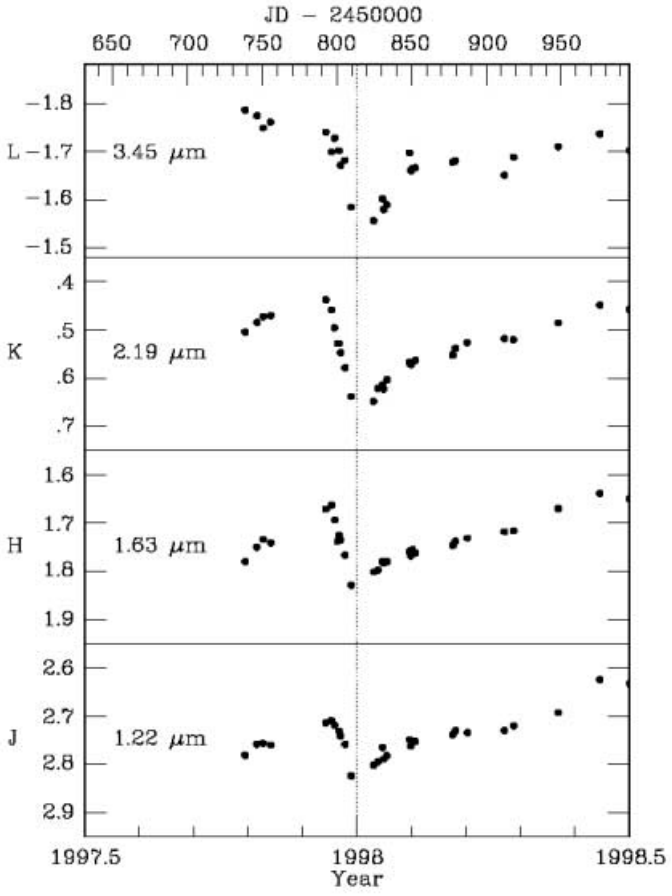

FIG. 9.—Fig. 4 from Feast et al. (2001), reproduced with permission of the authors. Infrared light curves in *JHKL* near the time of the 1998 dip. The minimum of the dip (phase 0.977) is shown by the vertical line.

[6] See http://lheawww.gsfc.nasa.gov/users/corcoran/eta_car/etacar_rxte_lightcurve.

Davidson et al. (1999a) discuss several possible explanations for the variability in the brightness of the central star of η Car. Since the star itself radiates near the Eddington limit, there is little room for rapid or dramatic changes in bolometric luminosity. This is supported by the fact that the surrounding nebula, which acts as a giant calorimeter for the central star, varies in brightness on a significantly smaller scale. If the bolometric luminosity of the central star stays roughly constant, then significant variations in its brightness may be more appropriately interpreted as changes in the density, temperature, and spatial distribution of intervening circumstellar material. An expanding shell of ejecta from an event may be able to produce the observed light curves (Zanella, Wolf, & Stahl 1984; Davidson et al. 1999a, 1999c; Smith et al. 2003). Any ejected shell should start hot with high opacities from ionized metals and then later shift these opacities to the red as the shell cools and dust forms. Particularly at early stages, this shell may be optically thin and as such would not have a significant impact on the continuum brightness.

The data show that the central star of η Car continues to brighten. We are unsure how long this trend can continue, but it appears to be driven by an increase in the apparent continuum brightness that may be caused by changes in the intervening circumstellar material along the line of sight, although how or why the circumstellar material may have been altered is not completely understood. Continued monitoring is critical, since coming out of the 2003.5 event there are indications that the central star may undergo another period of sudden dramatic brightening in the near future.

The brief decrease in the star's brightness during the 2003.5 event was more complicated than expected and changes preceding the event in the optical and near-UV started as early as 2003 January. The wavelength dependence of the dip indicates that it cannot be caused by a simple eclipse or occultation. If the primary star is eclipsed by the presumed secondary, we would expect to observe some decrease at all wavelengths, including the HRC/550M band that measures the continuum. On the other hand, if an eclipse of the secondary is sufficient to cause a dip of approximately 0.5 mag in the near UV flux of the central star, then we would expect to find some spectroscopic evidence of the secondary in the *HST* STIS spectra during the 5.5 yr cycle, which is not the case. However, the data may support a shell ejection model for the spectroscopic events. Additional data, including spectra gathered by the STIS during the 2003.5 event, should further constrain the mechanism powering these periodic phenomena.

This research was conducted as part of the *HST* Treasury Project on η Carinae via grant GO-9420 from the Space Telescope Science Institute. We acknowledge Kris Davidson, Roberta M. Humphreys, and Kazunori Ishibashi for directly assisting with the data and measurements and T. R. Gull for preparing most of the *HST* observing plans. Other participants in the *HST* Treasury Project are D. John Hillier, Augusto Damineli, Michael Corcoran, Otmar Stahl, Kerstin Weis, Sveneric Johansson, Fred Hamann, H. Hartman, Nolan Walborn, and Manuel Bautista. We are also grateful to the AAVSO International Database for the variable star observations contributed by observers worldwide. We individually thank Janet A. Mattei and Elizabeth O. Waagen of the AAVSO, who helped us obtain the data, and Stan Walker and R. Winfield Jones, who provided photoelectric photometry data. We are very appreciative of M. Feast and P. Whitelock for allowing us to reproduce their figures. We also, thank Matt Gray and Qian An for providing the η Carinae project with computer technical support.

REFERENCES

Altamore, A., Baratta, G. B., Cassatella, A., Rossi, L., & Viotti, R. 1986, in New Insights in Astrophysics, ed. E. J. Rolfe (Noordwijk: ESA), 303
Bingham, R. G., & Cousins, A. W. J. 1974, Mon. Notes Astron. Soc. South Africa, 33, 15
Cassatella, A., Giangrande, A., & Viotti, R. 1979, A&A, 71, L9
Clampin, M., Hartig, G., Baum, S., Kraemer, S. Kinney, E. Kutina, R., Pitts, R., & Balzano, V. 1996, STIS Instrument Science Report 96-030 (Baltimore: STSci)
Colina, L., Bohlin, R., & Castelli, F. 1996, Instrument Science Report CAL/SCS-008 (Baltimore: STSci)
Cousins, A. W. J. 1976, Mem. R. Astron. Soc., 81, 25
Damineli, A. 1996, ApJ, 460, L49
Davidson, K. 2000, in AIP Conf. Proc. 522, Cosmic Explosions, ed. S. S. Holt & W. W. Zhang (New York: AIP), 421
Davidson, K., et al. 1999a, AJ, 118, 1777
Davidson, K., & Humphreys, R. M. 1997, ARA&A, 35, 1
Davidson, K., Humphreys, R. M., Ishibashi, K., Gull, T. R., Hamuy, M., Berdnikov, L., & Whitelock, P. 1999b, IAU Circ., 7146, 1
Davidson, K., Ishibashi, K., Gull, T. R., & Humphreys, R. M. 1999c, in ASP Conf. Ser. 179, Eta Carinae at the Millennium (San Francisco: ASP), 227
Davidson, K., et al. 2004, in preparation
Davis, M., Campbell, D., Sticka, R., Faful, B. Leidecker, H., Kimbel, R., & Goudfrooij, P. 2001, STIS Failure Review Board Final Report (Baltimore: STSci)
Downes, R., Clampin, M., Shaw, R., Baum, S., Kinney, E., & McGrath, M. 1997, STIS Instrument Science Report 97-03B (Baltimore, STSci)
Feast, M., Whitelock, P., & Marang, F. 2001, MNRAS, 322, 741
Fernandez Lajus, E., Gamen, R., Schwartz, M., Salerno, N., Llinares, C., Farina, C., Amorn, R., & Niemela, V. 2003, Inf. Bull. Variable Stars, 5477, 1
Gull, T. R., Davidson, K., & Ishibashi, K. 2000, in AIP Conf. Proc. 522, Cosmic Explosions, ed. S. S. Holt & W. W. Zhang (New York: AIP), 439
Holtzman, J. A., Burrows, C. J., Casertano, S., Hester, J. J., Trauger, J. T., Watson, A. M., & Worthey, G. 1995, PASP, 107, 1065
Ishibashi, K., Davidson, M. F., Corcoran, K., Drake, S. A., Swank, J. H., & Petre, R. 1999, in ASP Conf. Ser. 179, Eta Carinae at the Millennium (San Francisco), 266
Johnson, H. L., & Morgan, W. W. 1951, ApJ, 114, 522
———. 1953, ApJ, 117, 313
Kim Quijano, J., et al. 2003, STIS Instrument Handbook, Ver. 7.0 (Baltimore: STScI)
Mattei, J. & Foster, G. 1998, IAPPP Commun., 72, 53
Mattei, J., & Fraser, B. 2003, J AAVSO, 31, 65
Pavlovsky, C., et al. 2003, ACS Instrument Handbook, Ver. 4.0 (Baltimore: STScI)
Proffitt, C. R. et al. 2002, in The 2002 *HST* Calibration Workshop, ed. S. Arribas, A. Koekemoer, & B. Whitmore (Baltimore: STScI), 97
Smith, N., Davidson, K., Gull, T. R., Ishibashi, K., & Hillier, D. J. 2003, ApJ, 586, 432
Sterken, C., de Groot, M. J. H., & van Genderen, A. M. 1996, A&AS, 116, 9
Sterken, C., Freyhammer, L., Arentoft, T., & van Genderen, A. M. 1999, A&A, 346, L33
———. 2001, in ASP Conf. Ser. 233, P Cygni 2000 (San Francisco: ASP), 39
van Genderen, A. M., Sterken, C., & Allen, W. H. 2003a, A&A, 405, 1057
van Genderen, A. M., Sterken, C., Allen, W. H., & Liller, W. 2003b, A&A, 412, L25
van Genderen, A. M., Sterken, C., de Groot, M., & Burki, G. 1999, A&A, 343, 847
Viotti, R., Rossi, L., Cassatella, A., Altamore, A., & Baratta, G. B. 1989, ApJS, 71, 983
Whitelock, P. A., Feast, M. W., Koen, C., Roberts, G., & Carter, B. S. 1994, MNRAS, 270, 364
Whitelock, P. A., Marang, F., & Crause, L. 2003, IAU Circ., 8160, 2
Zanella, R., Wolf, B., & Stahl, O. 1984, A&A, 137, 79